Progress In Electromagnetics Research M, Vol. 39, 193–201, 2014

Rayleigh Fading Channel Characterization Using K-Band FMCW Radar in Reverberation Chamber

Yun-Seok Noh, Rao S. Aziz*, Myung-Hun Jeong, Dae-Hwan Jeong, Ashwini K. Arya, and Seong-Ook Park

Abstract—This paper investigates the channel characterization of Rayleigh fading channel using K-band frequency-modulated continuous wave (FMCW) radar system. An IF (intermediate frequency) signal of K-band FMCW radar can be treated as time and frequency domain signals due to a unique property of linear frequency modulation (LFM). First, channel sounder FMCW radar stability has been confirmed by measuring power flatness of transmitted radio frequency signal and estimated range in anechoic chamber before conducting the experiment for channel characterization of Rayleigh fading channel. Next, the measurement setup has been conducted in reverberation chamber which emulates multipath fading phenomena. In reverberation chamber, four different cases have been examined by changing the boundary conditions inside it with and without flat microwave absorbers. This investigation leads to obtained scattered plots, normalized propagation delay profiles (PDPs), mean excess delay, root-mean-square (RMS) delay spread and envelope distribution of Rayleigh fading channel at about 24.591 GHz.

1. INTRODUCTION

Much research has been carried out since the International Telecommunication Union (ITU) approved the frequency of 24–24.25 GHz for long range radar (LRR) systems [1, 2]. Numerous researches have been done regarding frequency modulated continuous wave (FMCW) radar operation in K-band for distance measurement in multiple target situations. Moreover, continuous-wave operation makes FMCW radars less complex, thus cheaper and more reliable than pulse radars. These properties have caused the widespread use of FMCW radar technology for example in automotive applications [3]. Similarly, in rain radar and industry K-band, FMCW has many significant applications [4, 5]. At K-band, the attenuation due to rain effect may be noticeable, but it is weak enough to be correctable with sufficient accuracy.

Wireless communication system requires a channel sounder for the characterization of radio channel. In the past few decades, many researches have taken place on channel characterization by using different sounding techniques. The major purpose of channel sounding is to attribute a radio channel by decomposing the radio propagation path into its individual components [6]. In [7–9] radio channel is characterized by using vector network analyzer (VNA) as a measurement device. This technique is not cost effective but very sensitive because its accuracy strongly depends on the physical layout between the two ports. The scattering parameter (S_{21}) is only reliable for very close measurement when operating on higher frequency, as the movement of the cable such as bending can change the impedance of the cable [10]. In addition, due to time varying channels the measurement of channel frequency response can be changed, which leads to inaccurate impulse response measurement [11]. Another technique for channel sounding is pseudo random binary sequence radar which uses the spread spectrum technique. A

Received 28 October 2014, Accepted 18 November 2014, Scheduled 3 December 2014

* Corresponding author: Rao Shahid Aziz (rshahid@kaist.ac.kr).

The authors are with the Microwave and Antenna Laboratory, Department of Electrical Engineering, Korea Advanced Institute of Science and Technology (KAIST), 291 Daehak-ro, Yuseong-gu, Daejeon 305-701, Republic of Korea.

merit of this technique is that it has a strong immunity to noise signals and adjustable sensitivity by the control of chip length [11]. In time domain, it employs rectangular pulse which can be a *sinc* function in frequency domain. The *sinc*-like spectrum spreads in the frequency range [12] that is not suitable for observing the specific frequency band that needs to be used in [13]. An alternative but significant way for the characterization of channel frequency-modulated continuous (FMCW) radar has been utilized for channel sounding. Its system stability, repeatability and reliable measurement conditions [6, 14] are the reason for utilizing this method. Employing FMCW radar in [13–16] measurement of power delay profile (PDP), Doppler frequency, root mean square (RMS) delay spread, and channel capacity are successfully performed.

In this paper, FMCW radar is used for Rayleigh fading propagation channel characterization, and an intermediate frequency (IF) signal of FMCW radar is indicated in terms of both time and frequency domain signals based on the unique property of linear frequency modulation (LFM). The measurement is performed in reverberation chamber. Initially, the FMCW radar system stability has been investigated in the anechoic chamber by measuring the power flatness of transmitted radio signal and estimated range. After this, propagation measurement of Rayleigh fading channel is taken inside the reverberation chamber in multipath fading environment. Inside the reverberation chamber in a Rayleigh fading environment, four different cases with and without metallic absorbers are considered where the transmitting and receiving antennas are non-line-of-sight (NLOS). The PDPs are investigated by measuring the FMCW radar IF signals; a maximum delay time is determined. Mean excess delay times and RMS delay spreads are shown for four investigated cases and scatter plots of the measured IF signal are depicted. Furthermore, measured envelop distribution and theoretical ideal Rayleigh distribution are compared for the evaluation of the environment inside the reverberation chamber.

2. ANALYSIS OF FMCW RADAR SYSTEM AS A CHANNEL SOUNDER

The FMCW radar transmits a continuous radio wave frequency signal which is linearly swept. The transmitted signal hits the target and reflected back; therefore, the received signal is the combination of these two signals. The frequency difference between the transmitted and received signals of FMCW radar indicates a delay 'τ' due to the propagation distance of radio frequency signal. This frequency difference is called IF signal and denoted as S_{IF}. The IF signal can be utilized as a time domain signal as well as frequency domain signal, a unique property of linear frequency modulation (LFM). Figure 1 shows the generation of S_{IF} signal by mixing of transmitting (Tx) and receiving (Rx) antennas signals.

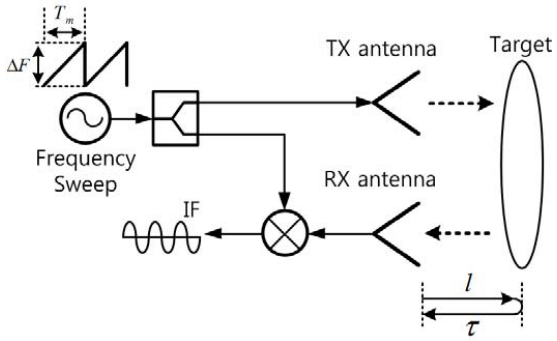

Figure 1. IF signal generation from Tx and Rx antennas.

Figure 2 shows the overall block diagram of the FMCW radar system. This system is the amalgamation of phase locked loops (PLLs) and a direct digital synthesizer (DDS) for linear frequency modulation (LFM), suitable for wideband performance. For coherent operation, PLLs and DDs are synchronized by one frequency source. RF-transmitter uses 56 MHz to generate 13.16 GHz signal. Similarly, RF-Receiver uses 56 MHz to generate 11.984 GHz signal. Moreover, baseband PLL uses 10 MHz frequency source to generate 1.872 GHz signal, whereas DDS uses 2.5 GHz signal. The frequency

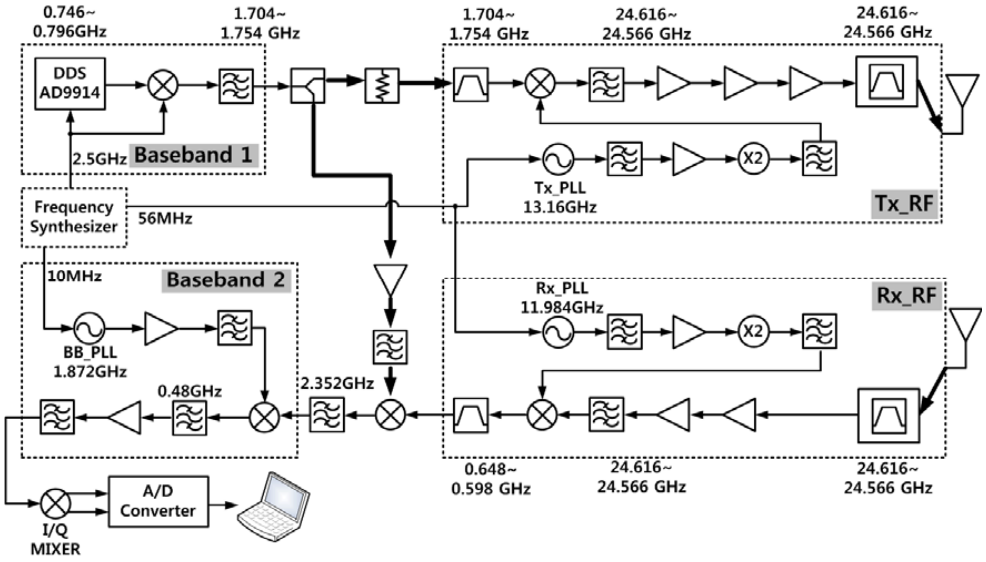

Figure 2. FMCW radar system block diagram.

sweep is modulated digitally by the DDS (AD9914) from 0.746 GHz to 0.796 GHz. In this measurement, the FMCW radar operating center frequency is 24.591 GHz. Also, the sweep bandwidth and time are 50 MHz and 385 µs, respectively.

In the LFM technique, the IF signal of the FMCW radar is interpreted in terms of time domain. It has already been investigated in [6] that the change of the sweep time corresponds to the change of the modulated frequency in the LFM; therefore, the time-domain signal in the slow modulation is represented in the frequency domain signal without Fourier transform algorithm. Hence, the scattering parameter S_{21} in the radio channel is proportional to the conjugate of the IF signal S_{IF} of the FMCW radar.

Consequently, the relationship between S_{21} and S_{IF} can be expressed as follows [6],

$$S_{21}\left(F_i\right) = k \cdot \left[S_{\mathrm{IF}}(F_t)\right]^*, \quad \left(t = \frac{i}{N-1} T_m\right) \tag{1}$$

where, k is an arbitrary constant, F_t the t-th frequency of IF signal, $*$ the conjugate operation, i the number of intervals, N the number of sweep frequencies in the sweep period, and T_m the modulation time of the FMCW radar.

The channel response can be extracted from the measured channel frequency response by performing an inversed discrete Fourier transform (IDFT) of S_{21} [17]. According to Eq. (1), the normalized impulse response (h_{norm}) of the radio channel using FMCW radar is defined by the discrete Fourier transform (DFT) of S_{IF}, because the IDFT of the S_{21} corresponds to the DFT of the S_{IF}. It can be written as [6],

$$h_{\mathrm{norm}}\left(\tau, m\right) = \frac{\mathrm{IDFT}\left[S_{21}\left(F_i, m\right)\right]}{\max\left(abs\left\{\mathrm{IDFT}\left[S_{21}\left(F_i, m\right)\right]\right\}\right)} = \frac{\mathrm{DFT}\left[S_{\mathrm{IF}}\left(F_i, m\right)^*\right]}{\max\left(abs\left\{\mathrm{DFT}\left[S_{\mathrm{IF}}\left(F_i, m\right)^*\right]\right\}\right)} \tag{2}$$

where, τ is the delay time and m the number of independent stirrer positions in the reverberation chamber.

Therefore, the normalized PDP can be defined by the impulse response as follows [8],

$$\mathrm{PDP}(\tau) = \frac{\left\langle \left|h_{\mathrm{norm}}\left(\tau, m\right)\right|^2 \right\rangle}{\max\left[\left\langle \left|h_{\mathrm{norm}}\left(\tau, m\right)\right|^2 \right\rangle\right]} \tag{3}$$

where, $\langle\,\rangle$ is the expectation operator.

3. EXPERIMENT AND RESULTS

3.1. Experiment Setup

The performance evaluation of K-band FMCW radar has been analyzed by examining the flatness of transmitted radio frequency signal and estimated range in anechoic chamber. The 24 GHz (K-band) standard gain horn antennas transmitting (Tx) and receiving (Rx) antennas are perfectly aligned to a circular metal target with a diameter of 25 cm. Figure 3 shows the experimental setup inside the anechoic chamber with Tx and Rx antennas, and the circular metal target. FMCW radar signal is generated by sweeping the DDS from 0.746 to 0.796 GHz, which measured using E4440A spectrum analyzer, and the result is reported in Figure 4(a), consisting of a 50 MHz bandwidth centered at 24.591 GHz. Figure 4(a) reveals that the transmitted power is very flat in the operating frequency domain. Furthermore, to extract frequency components, conventional fast Fourier Transform (FFT) algorithm has been applied.

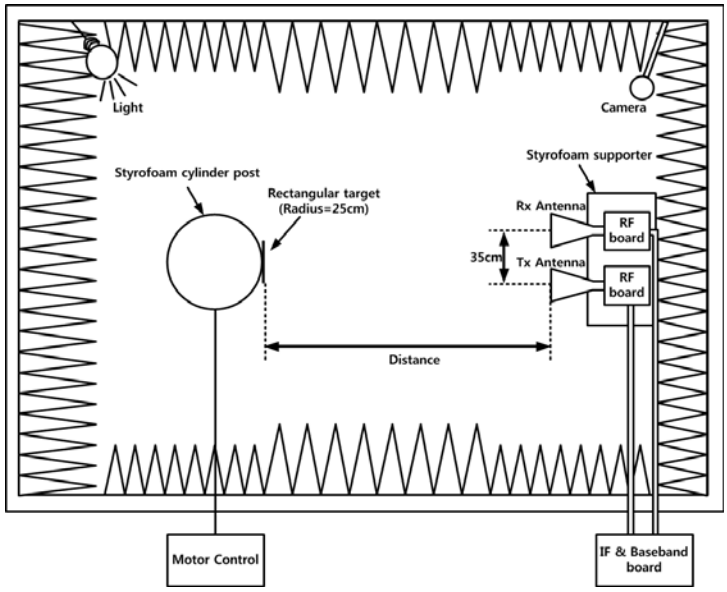

Figure 3. The experimental setup in the anechoic chamber.

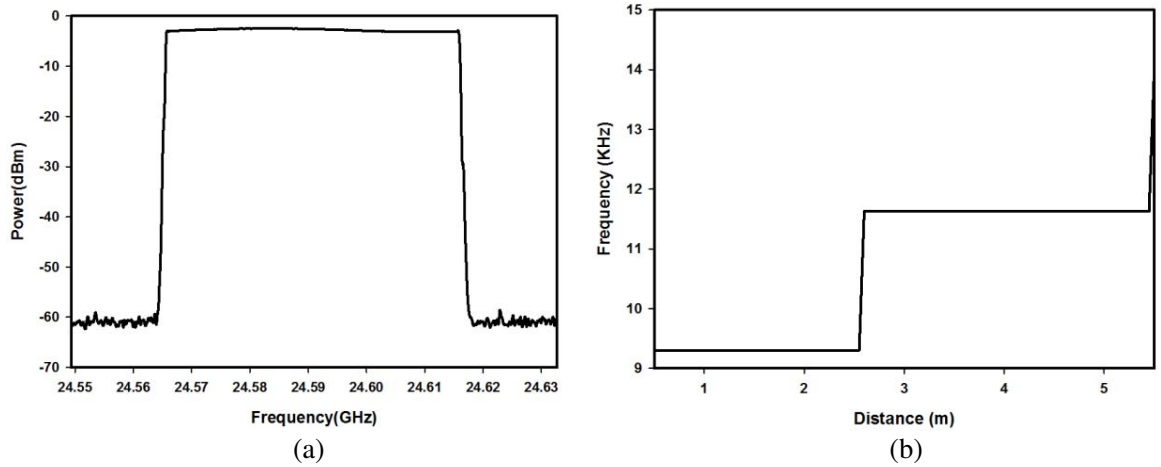

Figure 4. The performance evaluation of the proposed FMCW radar. (a) Flatness of transmitted RF signal. (b) Estimated range by FFT.

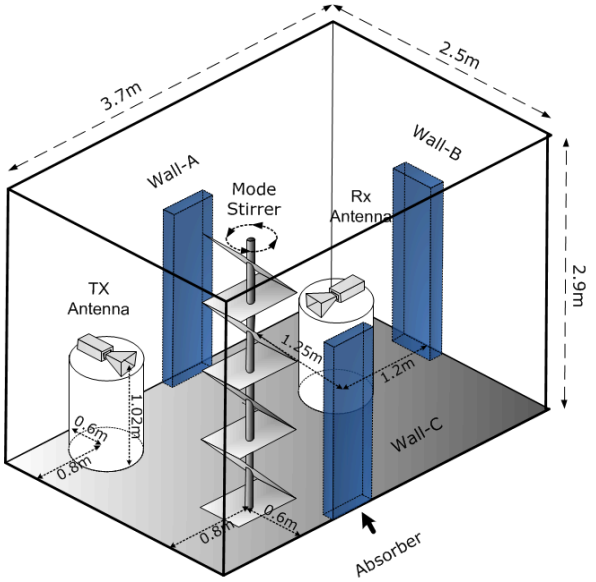

Figure 5. Measurement configurations in the reverberation chamber.

The range resolution of an FMCW radar is calculated and obtained by changing the distance of the target from 0.5 to 5.5 m, and also maximum peak of reflected wave can be found by utilizing FFT technique. Transmitted power flatness and range resolution confirm that the proposed K-band FMCW radar system operates properly.

In this experiment, the proposed FMCW radar is used as a channel sounder for K-band in the reverberation chamber which supports rich reflection. The dimension of the reverberation chamber is $2.5\,\mathrm{m}\,(W) \times 3.7\,\mathrm{m}\,(L) \times 2.9\,\mathrm{m}\,(H)$ with one mode stirrer in z-axis direction. The fundamental resonance frequency of reverberation chamber is about 72.4 MHz, and the lowest useable frequency (LUF) is about 350 MHz, enough for performance evaluation of 24 GHz channel. The three-dimensional measurement setup inside the reverberation chamber is depicted in Figure 5. It shows three different positions of flat microwave absorbers, mode stirrer, Tx, and Rx antenna systems. The 24 GHz Tx and Rx antennas for the FMCW radar are placed on the same plane, both K-band standard gain horn antennas have vertical polarization and 30° beamwidth. For investigating non-line of sight (NLOS) environment inside reverberation chamber, the Tx antenna is faced to the mode stirrer causes electromagnetic field waves to scatter randomly in the reverberation chamber. In contrary, the Rx antenna is orthogonally located to the Tx antenna to avoid direct radio path. The mode stirrer rotates in the counter clockwise (CCW) direction with 400 steps with step angle of 0.9° ($360°/400 = 0.9°$), and the number of sampled data is chosen as 1000 for each stirred position using the analog-to-digital converter.

For the investigation of K-band radio propagation under various radio environments, the microwave absorbers are placed at three different positions also shown in Figure 5. In our measurement, employed absorbers are laminated flat (AEL-4.5, Advanced Electromagnetic, Inc.) whose dimensions are $0.6\,\mathrm{m}\,(W) \times 0.11\,\mathrm{m}\,(L) \times 1.8\,\mathrm{m}\,(H)$. The detailed measurement setups for four different scenarios inside the reverberation chamber are specified in Table 1.

Table 1. Measurement setup for Rayleigh channel inside reverberation chamber.

Case	Absorber Position	Mode Stirrer Step Angle	Tm [μs]	Bandwidth [GHz]
1	None	$0.9°\ (=\frac{360°}{400})$	385	24.566 −24.616
2	A			
3	A, B			
4	A, B, C			

3.2. Experimental Results and Discussions

The scatter plot gives a true analysis of electromagnetic waves generated by the transmitting K-band antenna inside the reverberation chamber. Figure 6 shows the scatter plots of the measured intermediate frequency signal (S_{IF}) for four cases: 1, 2, 3, and 4 at 24.591 GHz. The boundary conditions of reverberation chamber can be changed by attaching the metallic microwave flat absorbers. It can be noticed that due to absorber attachment in Cases 2, 3, and 4, the measured IF signal is clustered in a circle located at the center of the origin which is considerably smaller than that of Case 1 in the absence of absorber. Due to the presence of absorbers, the transmitted signal in these cases decays rapidly compared to Case 1. This is because the measured S_{IF} signals are concentrated around the origin as direct coupling components between Tx and Rx antennas and are negligibly small compared to scattered components. Furthermore, it can be concluded that when more absorbers are attached to the metallic walls inside the reverberation chamber, the number of multipath components decreases which results in shrinking the scatter plot.

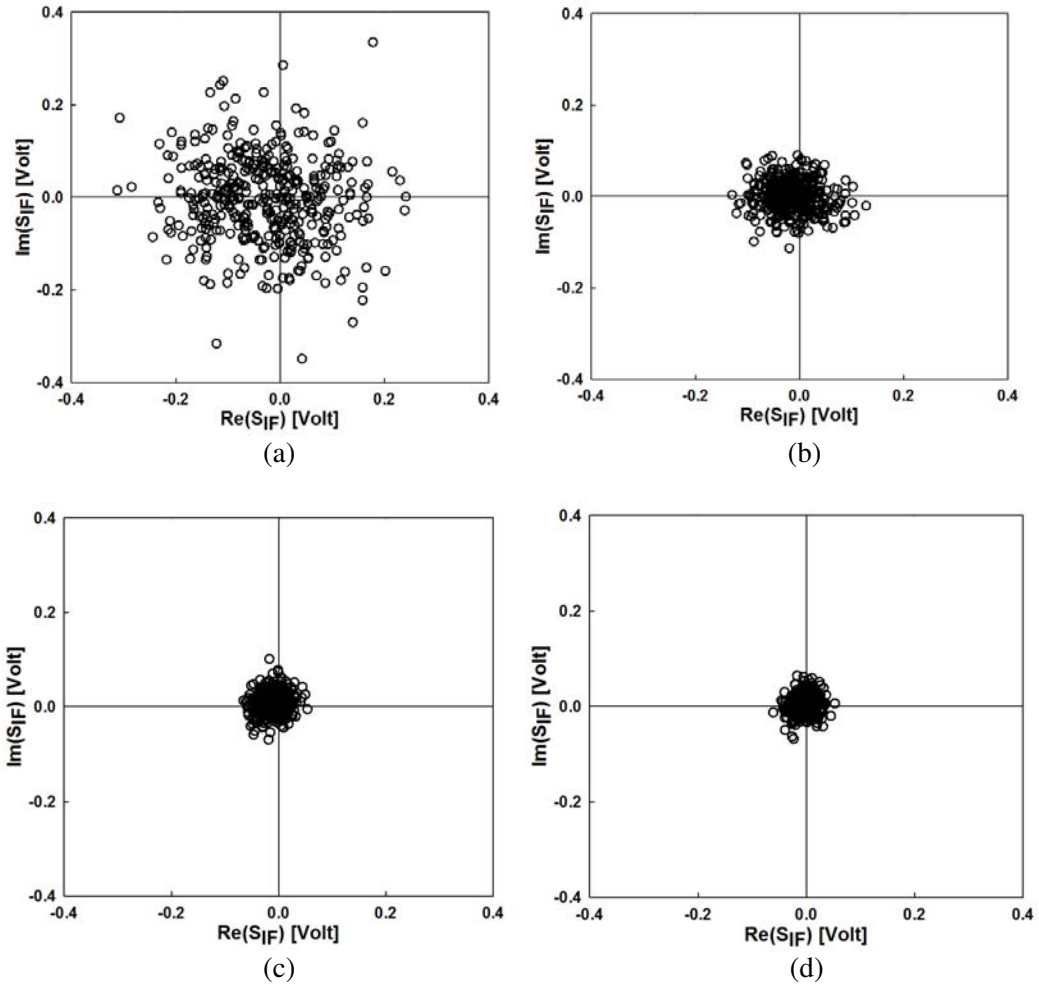

Figure 6. Scatter plots at 24.591 GHz. (a) Case 1. (b) Case 2. (c) Case 3. (d) Case 4.

The power delay profile (PDP) gives the intensity of a signal received through a multipath channel as a function of time delay. It is known from previous section that PDPs are obtained by taking the DFT of the measured S_{IF} signal of K-band FMCW radar. PDPs are shown in Figure 7, which are normalized by the maximum value of the Case 1 at 24.591 GHz. It can be seen in the 3D-plots that, as the received power decreased exponentially with the excess delay time, the decline slope becomes greater due to the

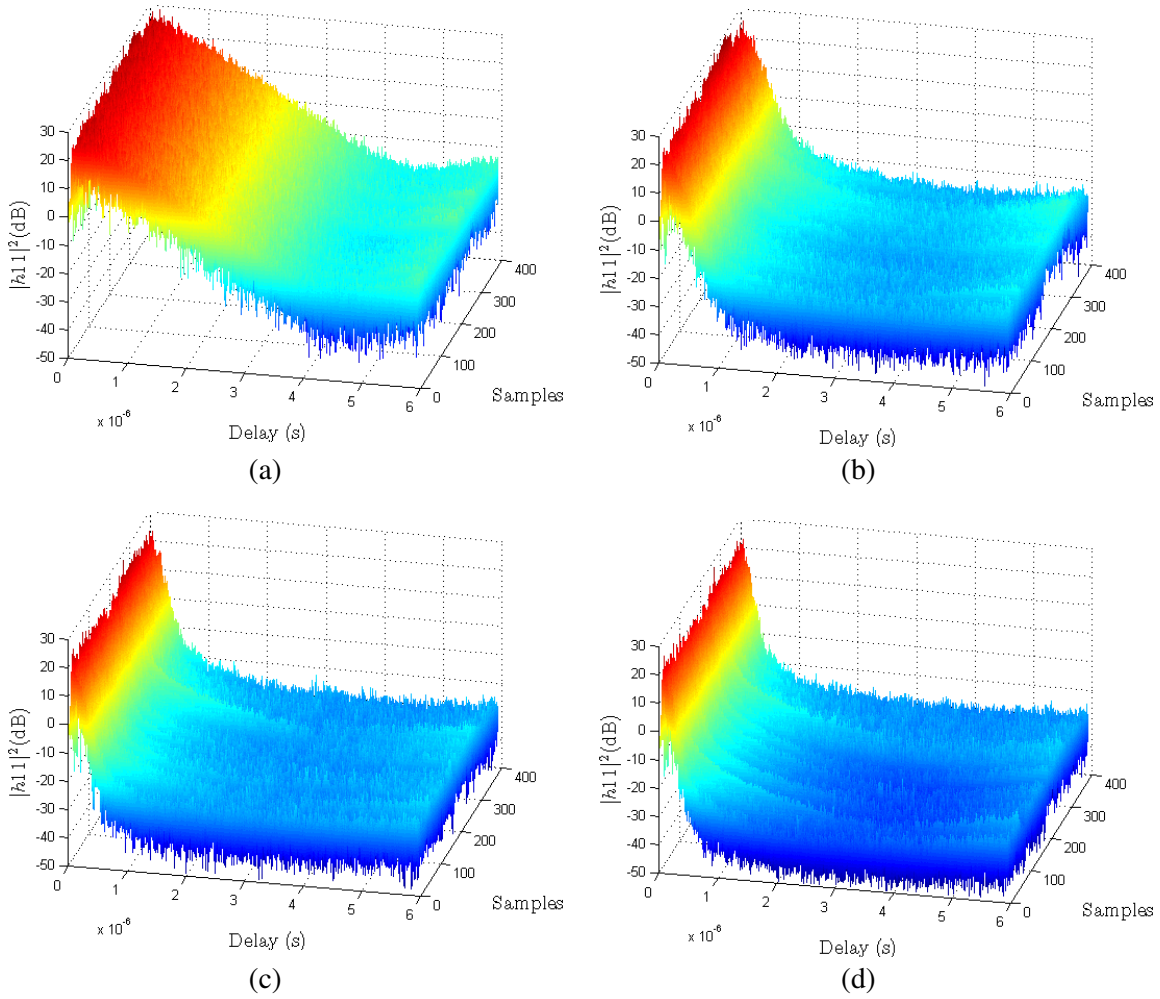

Figure 7. Normalized PDPs for Rayleigh fading channels. (a) Case-1. (b) Case-2. (c) Case-3. (d) Case-4.

Table 2. Mean excess delay times and RMS delay spreads.

Delay Time [μs]	Case			
	Case 1	Case 2	Case 3	Case 4
Mean Excess Delay	0.595	0.176	0.127	0.111
RMS Delay Spread	0.499	0.110	0.068	0.055

increase in the number of absorbers. After the excess delay time of 6 μs, the received power slowly decreases, and the PDPs becomes flat. The measured mean excess delay time and RMS delay spread for all the four cases are calculated and listed in Table 2. It is observed that in Case 1 without absorber, the obtained values are greater comparatively, whereas when the number of absorbers is increased, these values are noticeably decreased as the transmitted signal in the reverberation chamber decays rapidly.

The envelope distribution from Figure 6 is compared with the Rayleigh distributions. This plot is obtained by normalizing the measured S_{IF} over all mode stirrer positions at specific observation frequency. It is shown in Figure 8 that the multipath channels at K-band in NLOS propagation condition are emulated and dominant in the reverberation chamber, which is certainly well matched with the ideal Rayleigh fading distribution. Moreover, it can be concluded from Figure 8 that for all the cases, the probability density functions (PDFs) of the measured results are coherent with the Rayleigh

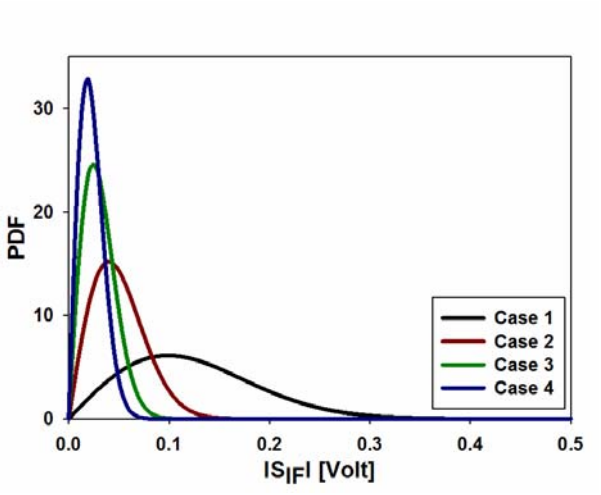

Figure 8. Envelope distribution at 24.591 GHz.

distribution. The Rayleigh parameters of Case 1 to Case 4 at 24.591 GHz are 0.0989, 0.0399, 0.0245 and 0.0184, respectively. In Case 1 in the absence of microwave absorber, the Rayleigh parameter has a larger value than other cases. It indicates that when the number of absorbers is increased, the Rayleigh parameter of envelope distribution is decreased.

4. CONCLUSIONS

In this paper we investigate the characteristic of radio propagation of Rayleigh fading channel at K-band in the reverberation chamber using frequency-modulated CW (FMCW) radar as a channel sounder. Initially, we analyze the performance evaluation of FMCW radar in anechoic chamber. The measured power flatness of transmitted radio frequency signal and estimated range in anechoic chamber shows that the radar operates properly and can be employed as a channel sounder for the propagation measurement of Rayleigh fading inside the reverberation chamber. In our study, we utilize the unique property of LFM, an IF signal (S_{IF}) of FMCW radar is presented in terms of the scattering parameter (S_{21}) and supports channel characteristics simultaneously in time and frequency domains. For the experiment setup inside the reverberation chamber we examine four different scenarios. The different scenarios are based on changing the metallic walls of the reverberation chamber, i.e., by attaching the flat metallic absorbers at different positions inside the reverberation chamber we have investigated multipath behavior. With this examination we have analyzed scattered plots, Power delay profiles and envelope distributions from the measured S_{IF} signal. Further, the obtained measured Rayleigh distribution in reverberation chamber is compared with the theoretical ideal Rayleigh distribution, which is certainly well matched with the ideal Rayleigh fading distribution. Similarly, mean excess delay and RMS delay spread for four different cases are measured and calculated from S_{IF}.

ACKNOWLEDGMENT

This research was financially supported by the National Research Foundation of Korea (NRF) grant funded by the Korea government (MSIP) (No. 2013R1A2A1A01014518) and by the Ministry of Education (MOE) and National Research Foundation of Korea (NRF) through Human Resource Training Project for Regional Innovation (NRF-2013H1B8A2032190).

REFERENCES

1. IEEE Standard Letter Designations for Radar-Frequency Bands, IEEE Std 521-2002 (Revision of IEEE Std 521-1984), 0–1, 3, 2003.

2. Leonid, A. B., M. S. Sergey, and N. K. Victor, *Handbook of RF, Microwave, and Millimeter-wave Components*, Artech House, 2012.
3. Klotz, M. and H. Rohling, "24 GHz radar sensors for automotive applications," *13th International Conference on Microwaves, Radar and Wireless Communications*, Vol. 1, 359–362, 2000.
4. Kneifel, S., M. Maahn, G. Peters, and C. Simmer, "Observation of snowfall with a low-power FMCW K-band radar (Micro Rain Radar)," *Meteorology and Atmospheric Physics*, Vol. 113, No. 1–2, 75–87, 2011.
5. Kaminski, P., K. Staszek, K. Wincza, and S. Gruszczynski, "K-band FMCW radar module with interferometic capability for industrial applications," *15th International Radar Symposium (IRS)*, 1–4, Jun. 2014.
6. Im, Y. T., M. Ali, and S. O. Park, "Slow modulation behavior of the FMCW radar for wireless channel sounding technology," *IEEE Transactions on Electromagnetic Compatibility*, No. 99, 1–9, 2014.
7. Chen, X., P.-S. Kildal, and S.-H. Lai, "Estimation of average Rician K factor and average mode bandwidth in loaded reverberation chamber," *IEEE Antennas Wireless Propag. Lett.*, Vol. 10, 1437–2011, Nov. 21, 2011.
8. Holloway, C. L., H. A. Shah, R. J. Pirkl, K. A. Remley, D. A. Hill, and J. Ladbury, "Early time behavior in reverberation chambers and its effect on the relationships between coherence bandwidth, chamber decay time, RMS delay spread, and the chamber buildup time," *IEEE Transactions on Electromagnetic Compatibility*, Vol. 54, No. 4, 714–725, Aug. 2012.
9. Holoway, C. L., D. A. Hill, J. M. Ladbury, P. F. Wilson, G. Koepke, and J. Coder, "On the use of reverberation chambers to simulate a Rician radio environment for the testing of wireless devices," *IEEE Trans. Antennas Propag.*, Vol. 54, No. 11, 3167–3177, Nov. 2006.
10. *PNA Millimeter-Wave Network Analyzers: Analysis of Cable Length on VNA System Performance*, Agilent Technologies, Santa Clara, CA, USA, 2004.
11. Rappaport, T. S., *Wireless Communications: Principles and Practice*, Chapter 4, Prentice-Hall, Englewood Cliffs, NJ, USA, 1999.
12. Cox, D. C., "Delay Doppler characteristics of multipath propagation at 910 MHz in a suburban mobile radio environment," *IEEE Trans. Antennas Propag.*, Vol. 20, No. 5, 625–635, Sep. 1972.
13. Feeney, S. M., "Wide-band channel sounding in the bands above 2 GHz," Doctoral Dissertation, Centre Commun. Syst., School Eng., Univ. Durham, Durham, U.K., 2007.
14. Salous, S., S. Feeney, N. Razvi-Ghods, and M. Abdalla, "Sounders for MIMO channel measurements," *European Signal Processing Conference*, Florence, Italy, Sep. 4, 2006.
15. Salous, S., P. Filippidis, R. Lewenz, I. Hawkins, N. Razavi-Ghods, and M. Abdallah, "Parallel receiver channel sounder for spatial and MIMO characterization of the mobile radio channel," *IEE Proc. Commun.*, Vol. 6, No. 152, 912–918, Dec. 9, 2005.
16. Salous, S. and H. Gokalp, "Dual-frequency sounder for UMTS frequency division duplex channels," *IEE Proc. Commun.*, Vol. 149, No. 2, 117–122, Apr. 2002.
17. Feeney, S. M. and S. Salous, "Implementation of a channel sounder for the 60 GHz band," *Proc. URSI XXIX Gen. Assem.*, Chicago, 2008.